



Available online at [www.sciencedirect.com](http://www.sciencedirect.com)



Applied Catalysis B: Environmental 74 (2007) 262–270



[www.elsevier.com/locate/apcatb](http://www.elsevier.com/locate/apcatb)

## Evaluation of catalytic properties of tungsten carbide for the anode of microbial fuel cells

Miriam Rosenbaum, Feng Zhao, Marion Quaas, Harm Wulff,  
Uwe Schröder\*, Fritz Scholz

Universität Greifswald, Institut für Biochemie, Felix-Hausdorff-Strasse 4, 17487 Greifswald, Germany

Received 22 December 2006; received in revised form 13 February 2007; accepted 13 February 2007

### Abstract

In this communication we discuss the properties of tungsten carbide, WC, as anodic electrocatalyst for microbial fuel cell application. The electrocatalytic activity of tungsten carbide is evaluated in the light of its preparation procedure, its structural properties as well as the pH and the composition of the anolyte solution and the catalyst load. The activity of the noble-metal-free electrocatalyst towards the oxidation of several common microbial fermentation products (hydrogen, formate, lactate, ethanol) is studied for microbial fuel cell conditions (e.g., pH 5, room temperature and ambient pressure). Current densities of up to  $8.8 \text{ mA cm}^{-2}$  are achieved for hydrogen (hydrogen saturated electrolyte solution), and up to  $2 \text{ mA cm}^{-2}$  for formate and lactate, respectively. No activity was observed for ethanol electrooxidation.

The electrocatalytic activity and chemical stability of tungsten carbide is excellent in acidic to pH neutral potassium chloride electrolyte solutions, whereas higher phosphate concentrations at neutral pH support an oxidative degradation.

© 2007 Elsevier B.V. All rights reserved.

**Keywords:** Tungsten carbide; Microbial fuel cell; Biofuel cell; Biohydrogen; Formate oxidation; Lactate

### 1. Introduction

Microbial fuel cells (MFC) are electrochemical devices that convert the chemical energy contained in organic matter into electricity by means of the catalytic (metabolic) activity of living microorganisms. They thus offer access to a direct generation of electricity from low-value biomass, such as agricultural wastes and sewage. This potential combination of waste treatment and power generation has led to a tremendously growing interest in microbial fuel cells and to substantial research progress, especially during the last 5–6 years.

Various MFC concepts have been proposed, and different mechanisms of the electron transfer from bacterial cells to the fuel cell anode have been discovered—and most likely, more will follow. Thus, a direct electron transfer between bacterial

membrane cytochromes and an electrode (e.g., graphite) is possible [1,2], although this process results only in low current densities. Some bacteria can form conducting nanowires (bacterial pili) to the anode as it has been supposed for *Shewanella oneidensis MR-1* [3] and *Geobacter sulfurreducens* [4], whereas other bacteria produce electron shuttling compounds like phenazines [5] to facilitate the electron disposal to a solid electron acceptor. It is likely that in mixed culture biofilms as they can be grown via electrochemical selection procedures [6–8], these different electron transfer mechanisms act in combination—resulting in a significantly increased current and power output.

Another approach is the direct oxidation of reduced, energy-rich metabolic products (primary metabolites) that are formed, e.g., during a fermentative substrate degradation. This approach differs from the above-mentioned concepts in that way that it requires robust electrocatalytic anodes that allow the efficient in situ oxidation of the microbial metabolites. An example for such anodes are sandwich electrodes composed of platinum as electrocatalyst, protected from poisoning reactions by an overlay of a conductive polymer [9,10]. These electrodes allow to very efficiently oxidize hydrogen, formed by fermentative

\* Corresponding author. Tel.: +49 3834 864330; fax: +49 3834 864451.

E-mail addresses: [miriam.rosenbaum@uni-greifswald.de](mailto:miriam.rosenbaum@uni-greifswald.de) (M. Rosenbaum), [zhao@uni-greifswald.de](mailto:zhao@uni-greifswald.de) (F. Zhao), [quaas@chemie.uni-greifswald.de](mailto:quaas@chemie.uni-greifswald.de) (M. Quaas), [wulff@chemie.uni-greifswald.de](mailto:wulff@chemie.uni-greifswald.de) (H. Wulff), [uwesch@uni-greifswald.de](mailto:uwesch@uni-greifswald.de) (U. Schröder), [fscholz@uni-greifswald.de](mailto:fscholz@uni-greifswald.de) (F. Scholz).

and phototrophic microbial cultures and from very different origin (glucose [10], starch and molasses [11], cellulose [12], light [13,14]), directly in bacterial solution.

The power density achievable with microbial fuel cells lies orders below that of chemical fuel cells. In order to be economical, the fuel cell components should be as inexpensive as possible—and the use of noble-metals like platinum should be avoided. For this reason, as well as for the liability of platinum towards poisoning and deactivation we have examined alternative electrocatalysts to replace platinum and to overcome its disadvantages.

For microbial fuel cell application, an electrocatalyst should possess the following features:

- good biocompatibility (no microbial toxicity),
- high electrocatalytic activity towards the oxidation of various metabolites,
- electrocatalytic activity at low temperatures (10–40 °C),
- electrocatalytic activity at pH between 5 and 7,
- chemical and electrochemical stability as well as high stability against biofouling,
- insensitivity against poisoning by biological products,
- low costs.

Recently, we have proposed a high performance, completely noble-metal-free, microbial fuel cell based on tungsten carbide as anodic electrocatalyst [15]. The results of that study indicate that tungsten carbide is excellently suitable as anodic electrocatalyst for MFC application. Thus, at graphite disc electrodes current densities of up to 3 mA cm<sup>-2</sup> were achieved in hydrogen saturated synthetic electrolytes (phosphate buffer). Further, a microbial fuel cell based on soil bacteria as biocatalysts and tungsten carbide as anodic electrocatalyst delivered the highest so far reported MFC power density of 586 μW cm<sup>-2</sup>.

Since the end of the 1960s, tungsten carbide has been discussed as alternative, robust and inexpensive electrocatalyst to substitute platinum as anodic fuel cell catalyst [16]. The investigation and development of this promising catalyst was, however, rather discontinuous, and the interest in tungsten carbide strongly faded at the end of the 1970s with the introduction of polymer electrolyte membrane fuel cells. Only recently – and probably caused by the heavily growing price of platinum – a certain revival of research into tungsten carbide by Chinese groups has taken place [17–20].

The preparation procedure of tungsten carbide is crucial for its electrocatalytic activity. Thus, different surface species and bulk phases have been found to decisively influence the electrocatalytic activity for hydrogen oxidation [17,21–26]. Summarising literature, three major surface processes determine the electrocatalytic activity of tungsten carbide: (i) the activation of tungsten carbide by the formation of oxidic surface groups that enhance the hydrogen adsorption process; (ii) the passivation (deactivation) by the formation of catalytically inactive tungsten oxide particles (corrosion), and (iii) the deposition of inactive elemental carbon particles during the preparation of tungsten carbide via carburization. A

variety of preparation and pre-treatment procedures have been proposed to obtain the most active tungsten carbide catalyst. As demonstrated later in this manuscript, some of these procedures were followed for this study.

Tungsten carbide possesses an excellent hydrogen oxidation performance at low costs. Unless platinum, however, WC is not inactivated by the strong platinum poisons hydrogen sulphide and carbon monoxide [27,28], but it can even effectively electrooxidize these compounds [22]. Further, tungsten carbide has been reported to possess a high catalytic activity towards the electrooxidation of a series of organic molecules as, for instance, formaldehyde, formic acid, acetaldehyde, propionaldehyde, acetylene and ethylene [22,27].

In this publication, we shall discuss the electrocatalytic properties of tungsten carbide under conditions of microbial fuel cells. The electrocatalytic activity of the catalyst towards the oxidation of several common microbial fermentation products like hydrogen, formate, ethanol and lactate has been examined in synthetic electrolyte solutions and under microbial fuel cell conditions (pH 7–5, room temperature and normal pressure). The influence of composition and pH of the electrolyte solutions is analysed as well as the catalyst's performance under microbial conditions of soil bacteria consortia and the role of the electrode backbone material.

## 2. Experimental details

### 2.1. Chemicals and materials

All chemicals were analytically pure and used as received. For comparative analyses commercial tungsten carbide from Strem Chemicals (WC 99.5%, particle size < 1 μm) was used. A perfluorinated membrane (Nafion<sup>®</sup> 117, DuPont) served as separator (diaphragm) in the electrochemical cell. As binder, a 5% Nafion<sup>®</sup> 117 solution was used.

Two different electrode materials were used as base materials (substratum) for catalyst deposition: polycrystalline sintered graphite in the form of graphite discs (Ø 4.9 mm, 0.19 cm<sup>2</sup> geometrical surface area) and graphite foil (ChemPur, Feinchemikalien und Forschungsbedarf GmbH, Karlsruhe; thickness 1 mm, geometric electrode area usually 1 cm × 1 cm). The polycrystalline graphite electrodes (for spectral analysis, Elektrokohle, Lichtenberg) were paraffin impregnated [29,30] in order to prevent a soaking with electrolyte solutions.

### 2.2. Catalyst and electrode preparation

Tungsten carbide was synthesized via high temperature carburization in a tube furnace. Two different preparation strategies have been applied:

WC I was prepared via the carburization of tungsten oxide, WO<sub>3</sub>, in a CO atmosphere at 800 °C according to Ref. [17]. Prior to syntheses, tungsten oxide was formed by dehydration of so-called yellow tungsten acid WO<sub>3</sub> × H<sub>2</sub>O at 500 °C under argon atmosphere for 1 h.

WC II was prepared similarly to WC I, but a powder mixture of pre-dried WO<sub>3</sub> with oxalic acid (H<sub>2</sub>C<sub>2</sub>O<sub>4</sub>) and NH<sub>4</sub>Cl was

used in a weight ratio of 4:2:1. The synthesis was performed at 750 °C [24,31].

All syntheses were performed in a carbon monoxide stream (flow rate: 10–15 L h<sup>-1</sup>) for 8–10 h at the respective temperatures. Carbon monoxide was synthesized by dropping dry formic acid into hot concentrated sulphuric acid with a dropping rate of 3–4 drops min<sup>-1</sup>. The CO gas stream was passed over solid KOH prior to entering the furnace in order to remove traces of water and carbon dioxide. After the synthesis, the product was allowed to cool down to room temperature under argon atmosphere.

For electrode preparation a defined amount of the tungsten carbide powder was mixed with Nafion<sup>®</sup> solution and hand-pressed onto a defined area of graphite foil or onto the graphite disc. The graphite foil was connected to the external circuit via a stainless steel wire.

### 2.3. X-ray analysis

The composition and morphology of the catalyst powder were determined by X-ray diffraction. X-ray powder patterns were recorded using a HZG 4 diffractometer (Seifert-FPM) in the Bragg-Brentano geometry. Cu K $\alpha$  radiation (40 kV and 40 mA) was applied and an angle range from 15 to 90°/2 $\theta$  was recorded at 0.02° increments and with 1 s counting time. The X-ray patterns were identified with the help of the PDF-2<sup>®</sup> X-ray database (International Centre for Diffraction Data, ICDD) referring to WC (#73-0471), hexagonal W<sub>2</sub>C (#79-0743), W (#04-0806) and WO<sub>2</sub> (#86-0314). The mean grain size was determined using the Scherrer equation:

$$D = \frac{k\lambda}{\beta_{\text{corr}} \cos\theta};$$

(with  $D$ , grain size;  $k$ , geometry factor,  $\lambda$ , wave length of exciting radiation,  $\beta_{\text{corr}}$ , full width at the half maximum (FWHM), corrected by an instrumental resolution width and  $\theta$  Bragg scattering angle).

### 2.4. Electron microscopy

Scanning electron microscopic images have been recorded using the scanning unit (SEI) of a JEM 1210, JEOL, (Tokyo, Japan) transmission electron microscope. Image processing was performed with the Link OXFORD processing software.

### 2.5. BET surface measurements

BET nitrogen adsorption measurements have been performed by Syntex GbR, Greifswald, using a Beckman-Coulter SA3100 instrument.

### 2.6. Electrochemical equipment and techniques

The electrochemical characterisation of the tungsten carbide anodes was carried out by potentiostatic, potentiodynamic and galvanodynamic methods either in 0.1 mol L<sup>-1</sup> potassium

chloride, 0.1 mol L<sup>-1</sup> phosphate buffer solution (0.05 mol L<sup>-1</sup> KH<sub>2</sub>PO<sub>4</sub> and 0.05 mol L<sup>-1</sup> K<sub>2</sub>HPO<sub>4</sub>) or in microbial growth medium (Section 2.5) using a conventional three electrode setup, with a platinum paddle as the counter electrode and a silver|silver chloride (sat. KCl; 0.197 V versus SHE) reference electrode. If not mentioned otherwise all potentials in this publication refer to this reference electrode. The experiments were carried out using PGSTAT20 and a PGSTAT30 potentiostats (Ecochemie, Netherlands). The latter was equipped with multi channel array modules for parallel recording of up to six working electrodes. The counter electrode was separated from the working electrode and the reference electrode by Nafion<sup>®</sup> membrane. The adjustment of the electrolyte pH was carried out with 2 mol L<sup>-1</sup> hydrochloric acid or sodium hydroxide and controlled with a glass electrode (Sensortechnik, Meinsberg, Germany).

### 2.7. Microbial experiments

Tungsten carbide modified electrodes were also studied under microbial fuel cell conditions, i.e., in microbial growth solutions. For this purpose, mixed microbial cultures were grown from selected spore forming microbes. For the selection process foliage and dung soil from the Botanical garden of the University of Greifswald was pre-treated at 120 °C for 2 h. Two grams of the sieved soil were inoculated into 250 mL culture medium (5 g glucose, 2 g NH<sub>4</sub>HCO<sub>3</sub>, 3.6 g KH<sub>2</sub>PO<sub>4</sub>, 0.1 g MgSO<sub>4</sub> per litre water; pH 6), nitrogen purged for 15 min and cultivated anaerobically at 37 °C [32].

## 3. Results and discussion

Fig. 1 shows the current versus time plot recorded during a batch experiment at a tungsten carbide modified graphite electrode immersed in a glucose substrate solution freshly inoculated with heat treated soil. The electrode was potentiostatically kept at a potential of 0.2 V (versus Ag/AgCl) to allow

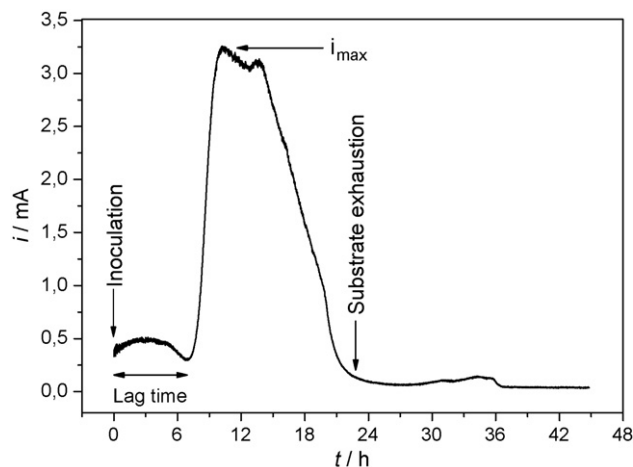


Fig. 1. Current generation in an anaerobic glucose substrate solution (5 g L<sup>-1</sup> glucose) inoculated with heat-treated soil (batch experiment). The working electrode was a WC modified graphite foil poised at a potential of 0.2 V, the temperature was 37 °C.

studying the anode performance unaffected by the cathode performance. The presented plot shows the typical features of the current generation using fermentative hydrogen producing cultures under batch conditions [11,32]. After inoculation with the biocatalyst (in this case spore containing heat treated soil) the bacterial culture requires a certain time span for germination and initial growth. As illustrated in Fig. 1 this lag time is 7 h for the soil-based biocatalyst under the applied experimental conditions. This is very short for a microbial fuel cell, especially in comparison to biofilm-based fuel cells. After 7 h the current strongly increases. As we have demonstrated in an earlier work, the increase of the current proceeds simultaneously with the exponential growths of the bacterial population [10]. The current maximum  $i_{\max}$  is reached when (i) the biocatalyst has reached its maximum activity (normally in the late logarithmic growth phase) and the rate of the formation of reduced electroactive metabolites reaches its maximum, or (ii) when the anode material has reached its oxidation capacity, i.e., the rate of metabolite oxidation becomes limiting. In order to achieve a high coulombic and energetic efficiency the electrocatalyst should be capable of oxidizing as many secondary metabolites as possible.

In the following paragraphs, we will emphasise the electrocatalytic properties of tungsten carbide with respect to its application as anode material for MFC application.

### 3.1. Dependence of the catalyst activity on its preparation, composition and structural properties

In Table 1, a summary is given of the catalyst samples used in this study and their properties, comprising the electrocatalytic activity towards the oxidation of dissolved hydrogen, the mean grain size, phase composition and relevant X-ray features. It has been frequently described that the electrocatalytic activity of

tungsten carbide strongly depends on its phase composition, morphology and surface properties [17,23,24]. As expected, the commercial tungsten carbide is not suitable as electrocatalyst material, as it possesses only a very low catalytic activity for hydrogen oxidation. Although consisting of a pure WC phase, maximum current densities of only  $160 \mu\text{A cm}^{-2}$  are obtained at graphite disc electrodes. This low activity can be attributed to the crystallinity (large intensities of the X-ray reflections, see Fig. 2 A) and a large average grain size of 107 nm leading to a comparatively low catalyst surface area of  $1.5 \text{ m}^2 \text{ g}^{-1}$  (BET measurement).

For the preparation of electrocatalytically active tungsten carbide we have chosen the comparably straightforward route via carburization of tungsten acid in a carbon monoxide stream. As described in Section 2.2 two slightly different preparation strategies were followed: (i) the preparation of ‘WC I’ from pure tungsten acid,  $\text{WO}_3 \times \text{H}_2\text{O}$ , and (ii) the synthesis of ‘WC II’ with addition of oxalic acid [31] for an increased surface area and the addition of  $\text{NH}_4\text{Cl}$  to prevent the formation of a passivating carbon layer on the catalyst surface [24]. The effect of chloride ions has been assigned to prevent the disproportionation of CO into carbon and  $\text{CO}_2$  during the carburization process [33].

In Fig. 2 the X-ray diffraction patterns of two tungsten carbide samples (A) commercial WC and (B) WC I/sample 01 (see Table 1) are presented. Both samples show only reflections of WC, with no visible fractions of  $\text{W}_2\text{C}$ , W or  $\text{WO}_2$ . As to be derived from the broader reflections and the lower peak intensities, the WC I sample 01 shows a considerably lower crystallinity than the commercial material. Table 1 summarizes the mean grain size of the samples (calculated from the X-ray patterns using the Scherrer equation). The grain size of all self prepared samples ranges between 10 and 20 nm, regardless of the preparation procedure. BET catalyst surface measurements

Table 1

X-ray powder diffraction characterisation of differently synthesized tungsten carbide samples and the characterisation of their electrocatalytic activity towards hydrogen oxidation

Sample <sup>a</sup>	$j_{\max}^b$ (mA cm <sup>-2</sup> ) (graphite disc)	Grain size <sup>c</sup> (nm)	Phase composition <sup>d</sup>	Molar ratio <sup>e</sup> WC/ (WC + W <sub>2</sub> C)	Molar ratio <sup>f</sup> WC/ (WC + W <sub>2</sub> C + W)	Peak Int <sup>f</sup> (P100)	Peak Int <sup>f</sup> (P101)	Ratio $I_{P100}/I_{P101}$
01 (WC I)	2.3	15	WC	1.00	1.00	308	338	0.911
02 (WC I)	1.1	11	WC	1.00	1.00	256	262	0.977
03 (WC I)	3.0	15	WC, W	1.00	0.85	399	399	1.000
04 (WC I)	1.8	19	WC, W	1.00	0.93	714	745	0.958
05 (WC II)	6.4	13	WC, W <sub>2</sub> C, W, WO <sub>2</sub>	0.77	0.62	295	285	1.035
06 (WC II)	2.0	19	WC, W	1.00	0.81	803	832	0.965
07 (WC II)	6.1	12	WC	1.00	1.00	331	311	1.064
08 (WC II)	8.8	13	WC, W <sub>2</sub> C, W	0.68	0.49	241	228	1.057
09 (WC II)	6.1	13	WC, W <sub>2</sub> C	0.80	0.80	358	358	1.000
Commercial WC <sup>g</sup>	0.16	107	WC	1.00	1.00	2455	2637	0.931

<sup>a</sup> Samples of consecutive preparations; different preparation procedures indicated with I and II (see Section 2.2).

<sup>b</sup> Limiting oxidation current determined from chronoamperometric experiments, measured in hydrogen saturated potassium chloride, 0.1 M, pH 5 at 0.2 V vs. Ag/AgCl, electrode substratum: graphite discs.

<sup>c</sup> Calculated from X-ray patterns using the Scherrer equation.

<sup>d</sup> Qualitative phase composition, determined using the PDF-2<sup>®</sup> X-ray database (International Centre for Diffraction Data, ICDD).

<sup>e</sup> Determined according to Ref. [25] from the X-ray diffraction patterns as  $x = h_1/(h_1 + h_2 + \dots)$ , with  $h$  being the heights of the most intensive reflections of the respective compounds.

<sup>f</sup> Peak intensities of the WC-100 and WC-101 reflexes.

<sup>g</sup> Strem Chemicals, 99.5% WC.

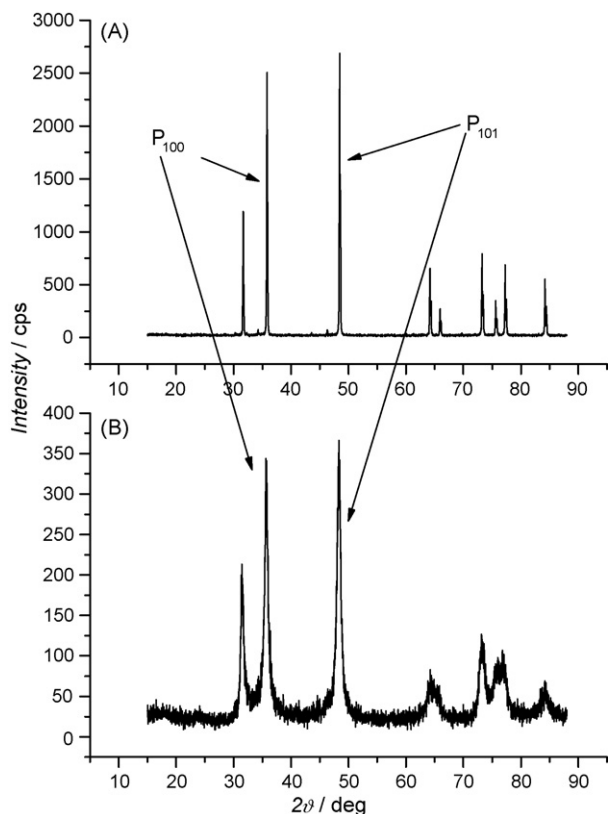


Fig. 2. X-ray diffraction patterns of (A) commercial WC, and (B) WC I sample 01

revealed a surface area of about  $8.5 \text{ m}^2 \text{ g}^{-1}$  for both self-synthesized catalyst types, WC I and WC II. Thus, we can state that the modified WC synthesis (addition of  $\text{NH}_4\text{Cl}$  and oxalic acid) did not have a significant effect on the grain size and the physical surface area. Fig. 3 shows scanning microscopic images of the commercial tungsten carbide, a WC I and a WC II sample (samples 02 and 07, respectively, Table 1). Most likely, the particulate structures of WC I and WC II depicted in Fig. 3B and C are not the individual tungsten carbide crystallites. They are, most probably, flakes consisting of crystallite aggregates. The SEM image of the commercial WC sample (Fig. 3A) shows single crystals as the average grain size (about 100 nm) is in good accordance with the imaged particle size. The smooth bulk surface of the presented commercial catalyst indicates a low degree of fine structuring.

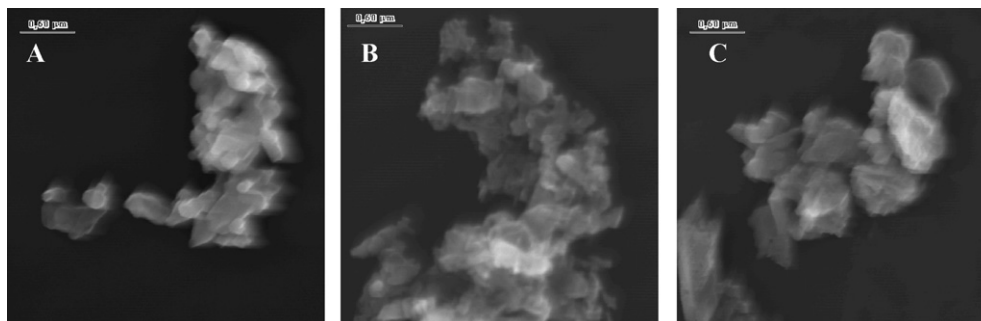


Fig. 3. SEM images of (A) commercial WC, (B) WC I sample 02, and (C) WC II sample 07 (SEI unit of TEM JEM 1210, JEOL).

The analysis of the X-ray patterns reveals a relatively strong variation of the sample composition. The major constituent of all samples is WC, however, most samples also contain various amounts of W and  $\text{W}_2\text{C}$  as side products of the reductive carburization.

WC II Sample 05 contains also  $\text{WO}_2$ , indicating an incomplete conversion of the reaction precursor. In order to estimate the molar fraction of WC in the catalyst samples the powder diffraction patterns of the samples were analysed with respect to the height of the most intensive reflections of identified compounds according to Vidick and co-workers [25]. This quantification represents only a rough approximation, since (i) the calculation relies on the peak heights rather than on the peak area and (ii) only the crystalline portions of the sample are measured. The deviating composition of the samples within the respective preparation procedure can most likely be attributed to the sensitivity of the reaction to variations in the flow rate of carbon monoxide.

As it is presented in Table 1, the activity for hydrogen oxidation of the self synthesized catalyst is considerably higher than of the commercial material, with an average current density of  $2.1 \text{ mA cm}^{-2}$  for the WC I catalyst and 5.9 for WC II. Besides the differences in the activity of both differently prepared catalyst materials it is noticeable that the catalytic activity greatly varies between the individual samples. As it can be seen from a comparison of samples 5, 7, 8 and 9, there is no significant correlation between the catalyst bulk composition and its electrocatalytic activity (limiting current densities for hydrogen oxidation). Despite of their varying composition all samples possess a comparable activity. Further, in spite of the generally lower WC content of the WC II samples compared to WC I it possesses a higher catalytic activity towards hydrogen oxidation.

A remarkable feature of all studied samples is a differently pronounced deviation of the ratio of peak intensities of the X-ray reflections at  $35.64^\circ$  and  $48.30^\circ$ . These signals correspond to the reflections of the WC-100 and WC-101 faces, respectively. Based on the WC #73-0471 data set of the PDF-2 X-ray database a ratio of 1.17 is to be expected for a statistically distributed tungsten carbide powder. All studied samples deviate from this value. The lower the ratio the higher is the deviation from the statistic distribution, indicating a certain texturing of the material, possibly caused by a deviation of the crystal shape from the statistical average. As depicted in

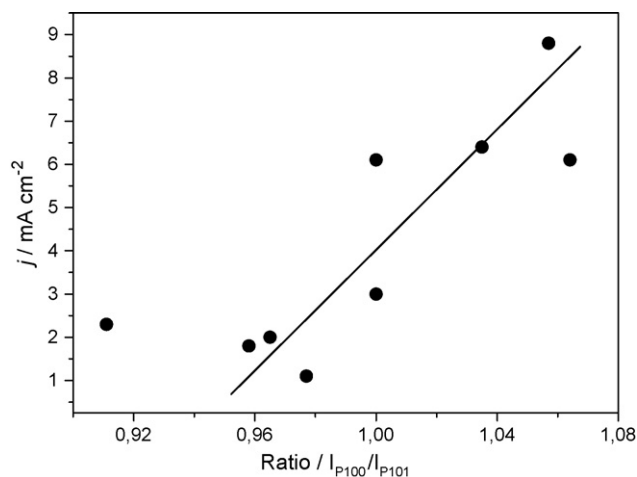


Fig. 4. Current density for the electrocatalytic hydrogen oxidation at all self-synthesized catalyst samples as a function of the ratio of the peak intensities of the WC-100 and WC-101 reflections.

Fig. 4, this has a distinct effect on the catalytic activity—the stronger the deviation from the statistical distribution the lower the electrocatalytic activity.

Summarizing the results of this section it can be stated that WC II, produced under the addition of oxalic acid and  $\text{NH}_4\text{Cl}$  to the carburization precursor mixture, possesses a considerably higher catalytic activity than WC I ( $5.9 \text{ mA cm}^{-2}$  versus  $2.1 \text{ mA cm}^{-2}$ ), which is in agreement to literature data. The grain size and the physical surface area of all samples is similar and no correlation can be derived between the catalytic activity and the phase composition. A texturing of the powder samples (deviation from the statistical distribution) appears to lead to a decreased electrocatalytic activity.

### 3.2. Electrocatalytic activity towards the oxidation of organic fermentation products

As it can be derived from Table 1, tungsten carbide possesses an excellent activity towards the electrooxidation of hydrogen. During microbial fermentation, however, only up to 4 mol of hydrogen per mole glucose are formed. This is a major restriction of dark fermentation, during which a number of other reduced fermentation products, especially organic acids and alcohols are formed.

In order to achieve a high energetic efficiency and substrate conversion, it is therefore of primary importance to access the organic fermentation products for direct oxidation and thus current generation. In our previous publication [15] we already mentioned the possibility of the electrooxidation of formate. Now, we studied the oxidation behaviour of formate, ethanol and lactate—major products of various fermentation pathways. To our knowledge, the electrooxidation of lactate at tungsten carbide has not been described before. So far, the possibility of the electrooxidation of carboxylic acids has even been denied [22,34].

Figs. 5 and 6 show the results of potentiodynamic (5) and galvanodynamic (Fig. 6) polarisation behaviour of tungsten carbide in the presence of formate and lactate. Both anolytes

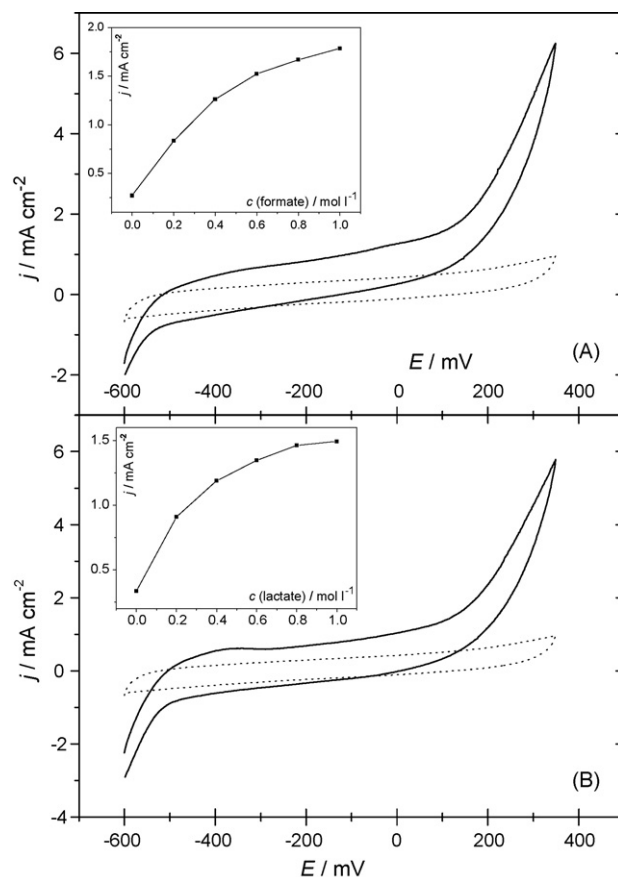


Fig. 5. Cyclic voltammograms of the oxidation of (A) formate and (B) lactate at tungsten carbide (WC II, sample 08, on a graphite foil electrode, catalyst load  $20 \text{ mg cm}^{-2}$ ). The experiments were performed at  $20^\circ\text{C}$ , in  $0.1 \text{ mol L}^{-1}$  stirred KCl, pH 5 with  $1 \text{ mol L}^{-1}$  anolyte concentration. The scan rate was  $2 \text{ mV s}^{-1}$ . Dotted lines: blank electrolyte, nitrogen purged. Inset: limiting current densities as a function of the concentration of the electroactive species, measured at  $0.2 \text{ V}$ .

possess a very similar oxidation behaviour—with current densities of up to  $2 \text{ mA cm}^{-2}$  obtained for lactate and formate at concentrations of  $1 \text{ mol L}^{-1}$ . Both experiments reveal that the oxidation of the two compounds is strongly potential dependent.

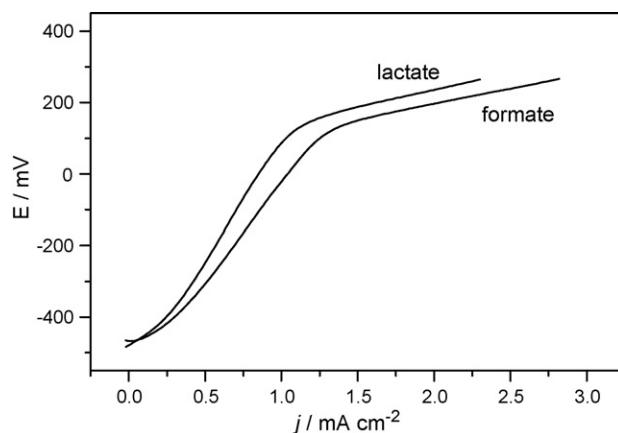


Fig. 6. Galvanodynamic polarisation curves of the electrocatalytic oxidation of formate and lactate at tungsten carbide. The experiment was at  $20^\circ\text{C}$ , in  $0.1 \text{ mol L}^{-1}$  stirred KCl, pH 5 with  $1 \text{ mol L}^{-1}$  anolyte concentration; the scan rate was  $5 \mu\text{A s}^{-1}$ .

Thus, Fig. 5 shows a strong increase of the current densities of the formate and lactate oxidation at approximately 150 mV, indicating a strong kinetic inhibition at lower redox potentials. An explanation was proposed by Benda et al., who suggested that at low current densities the electrooxidation of formic acid proceeds via the oxidation of hydrogen evolved in the decomposition of formic acid, while at higher current densities a direct oxidation of formic acid is possible [22]. Although these results were obtained from experiments performed under strongly acidic conditions (1 M sulphuric acid) and mechanisms might be different at pH 5, these results give a first indication for the mechanisms of formate and lactate oxidation at neutral (or only slightly acidic) pH. We could find support for this mechanism by galvanodynamic measurements (data not shown) of the electrocatalytic hydrogen oxidation, which at low current densities results in very similar slopes of the polarization curves in comparison to formate and lactate oxidation.

We also studied the electrocatalytic properties of the catalyst towards the oxidation of ethanol, a major fermentation product. Here, we have to confirm the results of other studies, e.g., for the oxidation of methanol [27], that tungsten carbide shows no significant activity towards oxidation of alcohols.

### 3.3. Influence of the composition and the pH of the electrolyte solution on the catalytic activity and the stability of tungsten carbide

So far, the electrocatalysis at tungsten carbide had been mainly studied under strongly acidic conditions. Already in 1972, Benda et al. examined the catalyst's properties in 1 mol L<sup>-1</sup> sulphuric acid, 14 mol L<sup>-1</sup> phosphoric acid and 6 mol L<sup>-1</sup> potassium hydroxide [22]. Only recently, Ma et al. published a comparative study of the oxidation stability of WC in sulphuric and hydrochloric acid as well as potassium hydroxide [18]. In the first study, the highest stability and activity of the catalyst was achieved in sulphuric acid. In phosphoric acid, a similar catalytic behaviour was observed, but considerably lower current densities were achieved. In alkaline electrolyte solutions the catalytic behaviour differed significantly. A corrosion current was found, which is also observed for short times at freshly prepared tungsten carbide in acidic solutions, and which leads to a steady degradation of the catalyst layer.

Fig. 7 illustrates the effect of a pH variation and a varying electrolyte composition on the electrocatalytic oxidation of hydrogen at tungsten carbide and on the stability of the electrocatalyst. In this figure the pH of two hydrogen saturated electrolyte solutions (A) 0.1 M KCl, and (B) 0.1 M KH<sub>2</sub>PO<sub>4</sub>/K<sub>2</sub>HPO<sub>4</sub> was stepwise decreased from neutral to acidic conditions with the oxidation current measured at a fixed potential of 0.2 V. In the case of the potassium chloride electrolyte, the catalytic activity of tungsten carbide does not significantly depend on the solution pH. At the tungsten carbide modified graphite foil electrode an average current density of about 1 mA cm<sup>-2</sup> is achieved in a pH range between 1 and 7. In comparison to the measurements performed on polycrystalline

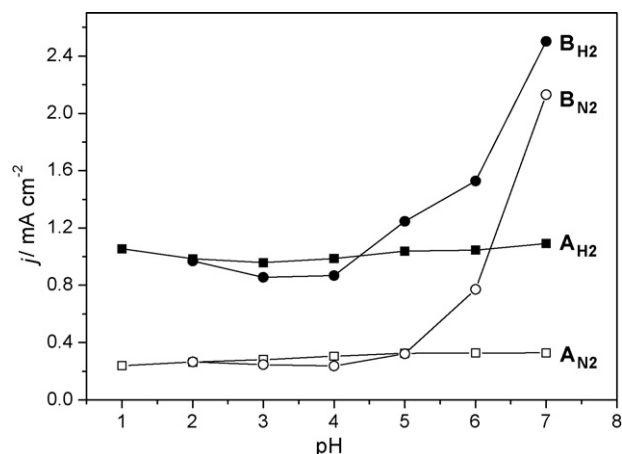


Fig. 7. Dependence of the current densities of the electrocatalytic hydrogen oxidation (solid symbols) at tungsten carbide on the pH of the electrolyte solution: (A) 100 mM KCl, (B) 100 mM phosphate buffer (open symbols give base current in N<sub>2</sub> purged electrolyte). The electrode was polarized at 0.2 V vs. Ag/AgCl, sat. KCl (electrode: catalyst WC II, sample 05, 20 mg cm<sup>-2</sup>, at graphite foil electrode). All solutions were stirred.

graphite the current density is significantly lower. This effect of the electrode substratum will be discussed later (Section 3.4).

In the phosphate buffer solution (Fig. 7, curve B) the behaviour of tungsten carbide differs from that in chloride solution. Whereas at a pH below 5 the current density is slightly lower (0.8 mA cm<sup>-2</sup>) than that obtained in KCl, the current increases significantly at more neutral pH values.

As shown in Fig. 7 (curve 7 B<sub>N2</sub>), this effect is independent of the presence of the anolyte (fuel). Thus, the current increase is not caused by an increasing catalytic activity but by a corrosive oxidation of the catalyst. Thus, it has been reported that under acidic conditions tungsten carbide is oxidized at potentials higher than 900 mV (versus dynamic hydrogen electrode, DHE). An unstable, blue tungsten oxide is formed, which is further oxidized at higher potentials [18]. The corrosion potential of tungsten carbide is shifted towards negative values at alkaline pH (solubilisation of the formed tungsten oxide by the formation of soluble tungstates). It is likely, that in a pH neutral phosphate buffer solution the formation of soluble phosphor-tungstic acids shifts the corrosion potential towards more negative potentials, which leads to an irreversible degradation of the catalyst even at potentials as low as 0.2 V.

For the use of tungsten carbide as anodic microbial fuel cell electrocatalyst such behaviour is not favourable. However, since most MFCs are usually operated at slightly acidic pH conditions and at a considerably lower concentration of phosphate ions, this effect is avoidable.

### 3.4. Influence of the electrode substratum and the catalyst load

In our preceding study, we used graphite disc electrodes fabricated from sintered polycrystalline graphite as electrode base material for the study of tungsten carbide as microbial fuel cell electrocatalyst [15]. These electrodes are ideal for

fundamental electrochemical studies [29,30] but due to their small size they are rather unsuitable for practical application. Finding a suitable electrode base material (substratum), however, is not trivial, since the substratum itself may play an important role in the electrooxidation performance [35]. In previous studies, we have successfully used graphite foil produced from flaked natural graphite as base material for electrocatalytic oxygen reduction at pyrolysed transition metal porphyrines and phthalocyanines [36,37]. The results obtained at graphite foil were comparable with those measured at the polycrystalline graphite disc electrodes. The same applies for the electrooxidation of formate and lactate at tungsten carbide. Here, the results obtained at the graphite foil electrodes are comparable with those at the polycrystalline graphite (data not shown). As Fig. 8 shows, however, this does not apply to the electrocatalytic oxidation of hydrogen at tungsten carbide. In Fig. 8 the limiting current densities of the electrocatalytic hydrogen oxidation at different self-synthesised catalyst samples, immobilized either at polycrystalline graphite or at graphite foil, are plotted. Clearly visible is the considerably better performance of the graphite disc electrodes. On the average, the current densities achievable at these electrodes are six times larger than at graphite foil.

Presently, we are not able to interpret this peculiar behaviour, which, as Fig. 8 illustrates, applies to all studied catalyst samples. However, considering the differing structure of the electrode materials such effect may not sound surprising. The relatively poor performance of graphite foil may be attributed to its layered structure: The graphite layers are arranged parallel to the foil surface, and any electron flow perpendicular to the layers – like the electron transfer from tungsten carbide to the carbon backbone – is hampered by an increased resistance. This anisotropy can be read off from macroscopic data like the specific resistance, which is about seventy times larger perpendicular to the graphite layers than parallel. Instead, a surprising fact is, that despite of this anisotropy, we get equivalent results on both substrates for the oxygen reduction catalysts or the oxidation of other anodic fuels.

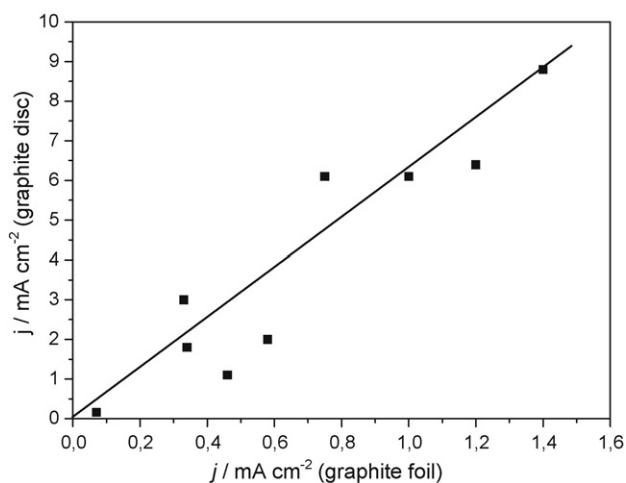


Fig. 8. Correlation of the limiting current densities for the electrocatalytic oxidation of dissolved hydrogen at different catalyst samples immobilised at polycrystalline graphite and at graphite foil.

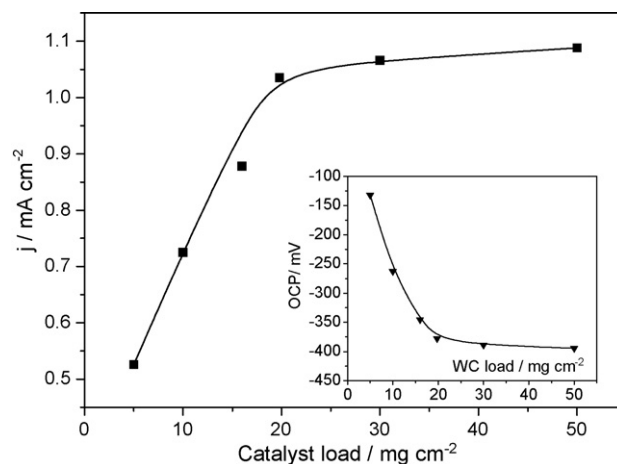


Fig. 9. Current densities as function of the catalyst load. Data are derived from galvanodynamic polarisation experiments at 0.2 V (sweep rate  $5 \mu\text{A s}^{-1}$ ) performed in a fermented anaerobic culture of soil bacteria. The solution was stirred and hydrogen purged. Parallel investigations of six graphite foil electrodes with the respective amount of catalyst. Inset: open circuit potential (OCP) as a function of the catalyst load.

Fig. 9 depicts the dependence of the electrocatalytic performance of tungsten carbide modified electrodes on the catalyst load in hydrogen saturated, readily fermented glucose medium. The experiment was performed in the following way: a glucose medium inoculated with hydrogen producing soil was anaerobically incubated at  $37^\circ\text{C}$  [32]. Six electrodes with different catalyst loads (catalyst WC II sample 07) were immersed in the bacterial culture and polarized at 0.2 V in order to oxidize bacterial fermentation products. After 48 h hydrogen was bubbled into in the exhausted medium in order to measure the electrode activity under hydrogen saturated conditions and to register potential activity losses that may have occurred over the operation time. Fig. 9 shows that the current density increases considerably up to a catalyst load of  $20 \text{ mg cm}^{-2}$ . Higher loads lead only to a slight further improvement of the performance.

A comparison of the performance data in Fig. 9 to the current density of freshly prepared electrodes (e.g., the limiting current density for a catalyst load of  $20 \text{ mg cm}^{-2}$  is  $1.0 \text{ mA cm}^{-2}$ ) proves the high stability of the catalyst, with no sign of degradation or deactivation processes. The results obtained at the polycrystalline graphite disc electrodes are similar, however, at an average current density six times larger than at graphite foil.

First preliminary experiments indicate that the proportion of maximum current density per catalyst load can be further increased by diluting the catalyst with a nanocrystalline carbon (Vulcan XC72, Cabbot). However, the differences between the polycrystalline graphite electrodes and the graphite foil remain. Further studies are planned to address these important questions.

#### 4. Conclusion

As a result of this study it can be stated that tungsten carbide is a promising MFC electrocatalyst that is capable of efficiently oxidizing common fermentation products like hydrogen, formate and lactate under the conditions of microbial fuel

cells. Yet, a number of important issues are to be addressed in further studies. Major priority is the optimisation of the preparation procedure to yield highly active tungsten carbide. Our results suggest that occurring deviations of the X-ray powder diffraction patterns from the statistic distribution may serve as an indicator for a first prediction of the electrocatalytic activity. Here, however, more work will be necessary to clarify the cause of these deviations.

Further emphasis will be put on the study of the electron transfer between tungsten carbide and the electrode support. Depending on the electrode material this electron transfer seems to represent a major bottleneck confining the electrocatalytic activity of tungsten carbide modified electrodes.

### Acknowledgement

U.S. and F.Z. thank the Deutsche Forschungsgemeinschaft (DFG). U.S., M.R. and F.S. acknowledge support by Fonds der Chemischen Industrie. We gratefully acknowledge the help Mr. Manfred Zander for the conduction of the electron microscopy.

### References

- [1] D.R. Bond, D.E. Holmes, L.M. Tender, D.R. Lovley, *Science* 295 (2002) 483–485.
- [2] S.K. Chaudhuri, D.R. Lovley, *Nat. Biotechnol.* 21 (2003) 1229–1232.
- [3] Y.A. Gorby, S. Yanina, J.S. McLean, K.M. Rosso, D. Moyles, A. Dohnalkova, T.J. Beveridge, I.S. Chang, B.H. Kim, K.S. Kim, D.E. Culley, S.B. Reed, M.F. Romine, D.A. Saffarini, E.A. Hill, L. Shi, D.A. Elias, D.W. Kennedy, G. Pinchuk, K. Watanabe, S.I. Ishii, B. Logan, K.H. Nealson, J.K. Fredrickson, *PNAS* 103 (2006) 11358–11363.
- [4] G. Reguera, K.P. Nevin, J.S. Nicoll, T.L. Woodard, D.R. Lovley, *Appl. Environ. Microbiol.* 72 (2006) 7345–7348.
- [5] K. Rabaey, N. Boon, S.D. Siciliano, M. Verhaege, W. Verstraete, *Appl. Environ. Microbiol.* 70 (2004) 5373–5382.
- [6] B.H. Kim, H.S. Park, H.J. Kim, G.T. Kim, I.S. Chang, J. Lee, N.T. Phung, *Appl. Microbiol. Biotechnol.* 63 (2004) 672–681.
- [7] H. Liu, R. Ramnarayanan, B.E. Logan, *Environ. Sci. Technol.* 38 (2004) 2281–2285.
- [8] K. Rabaey, G. Lissens, S.D. Siciliano, W. Verstraete, *Biotechnol. Lett.* 25 (2003) 1531–1535.
- [9] J. Nießen, U. Schröder, M. Rosenbaum, F. Scholz, *Electrochem. Commun.* 6 (2004) 571–575.
- [10] U. Schröder, J. Nießen, F. Scholz, *Angew. Chem. Int. Ed.* 115 (2003) 2986–2989.
- [11] J. Nießen, U. Schröder, F. Scholz, *Electrochem. Commun.* 6 (2004) 955–958.
- [12] J. Nießen, U. Schröder, F. Harnisch, F. Scholz, *Let. Appl. Microbiol.* 41 (2005) 286–290.
- [13] M. Rosenbaum, U. Schröder, F. Scholz, *Environ. Sci. Technol.* 39 (2005) 6328–6333.
- [14] M. Rosenbaum, U. Schröder, F. Scholz, *Appl. Microbiol. Biotechnol.* 68 (2005) 753–756.
- [15] M. Rosenbaum, F. Zhao, U. Schröder, F. Scholz, *Angew. Chem. Int. Ed.* 45 (2006) 6658–6661.
- [16] H. Böhm, F.A. Pohl, *Wiss. Ber. AEG-Telefunken* 41 (1968) 46.
- [17] C. Ma, W. Zhang, D. Chen, B. Zhou, T. Nonferr. Met. Soc. 12 (2002) 1015–1019.
- [18] C. Ma, Y. Gan, Y. Chu, H. Huang, D. Chen, B. Zhou, T. Nonferr. Met. Soc. 14 (2004) 11–14.
- [19] X.G. Yang, C.Y. Wang, *Appl. Phys. Lett.* 86 (2005) 1–3.
- [20] H.J. Zheng, J.G. Huang, W. Wang, C.N. Ma, *Electrochem. Commun.* 7 (2005) 1045–1049.
- [21] H. Böhm, *Electrochim. Acta* 15 (1970) 1273–1280.
- [22] K.V. Benda, H. Binder, A. Köhling, G. Sandstede, in: G. Sandstede (Ed.), *From Electrocatalysis to Fuel Cells*, The University of Washington Press, Seattle, 1972.
- [23] R. Fleischmann, H. Böhm, *Electrochim. Acta* 22 (1977) 1123–1128.
- [24] P.N. Ross Jr., P. Stonehart, *J. Catal.* 48 (1977) 42–59.
- [25] B. Vidick, J. Lemaitre, B. Delmon, *J. Catal.* 99 (1986) 428–438.
- [26] P. Zoltowski, *Electrochim. Acta* 31 (1986) 103–111.
- [27] V.S. Palanker, R.A. Gajjev, D.V. Sokolsky, *Electrochim. Acta* 22 (1977) 133–136.
- [28] D.R. McIntyre, G.T. Burstein, A. Vossen, *J. Power Sources* 107 (2002) 67–73.
- [29] F. Scholz, B. Meyer, *Voltammetry of Solid Microparticles Immobilized on Electrode Surfaces*, Marcel Dekker, Inc., New York, Basel, Hong Kong, 1998.
- [30] F. Scholz, U. Schröder, R. Gulaboski, *Electrochemistry of Immobilized Particles and Droplets*, Springer, Berlin, Heidelberg, New York, 2005.
- [31] D. Baresel, W. Gellert, J. Heidemeyer, P. Scharner, *Angew. Chem. Int. Ed.* 10 (1971) 194–197.
- [32] J. Nießen, F. Harnisch, M. Rosenbaum, U. Schröder, F. Scholz, *Electrochem. Commun.* 8 (2006) 869–873.
- [33] I. Nikolov, M. Svata, L. Grigorov, T. Vitanov, Z. Zabransky, *J. Power Sources* 3 (1978) 237–244.
- [34] H. Binder, A. Köhling, W. Kuhn, G. Sandstede, *Angew. Chem. Int. Ed.* 8 (1969) 757–758.
- [35] T.J. Davies, M.E. Hyde, R.G. Compton, *Angew. Chem. Int. Ed.* 44 (2005) 5121–5126.
- [36] F. Zhao, F. Harnisch, U. Schröder, F. Scholz, P. Bogdanoff, I. Herrmann, *Electrochem. Commun.* 7 (2005) 1405–1410.
- [37] F. Zhao, F. Harnisch, U. Schröder, F. Scholz, P. Bogdanoff, I. Herrmann, *Environ. Sci. Technol.* 40 (2006) 5191–5199.